**SLOPE - GEOLOGIC AGE RELATIONSHIPS IN COMPLEX LUNAR CRATERS** C. Rojas[1], P. Mahanti[1], M. S. Robinson[1], LROC Team[1], [1]LROC Science Operation Center, School of Earth and Space Exploration, Arizona State University, Tempe, Arizona (crojas@ser.asu.edu)

**Introduction:** Impact events leading to formation of basins and large craters dominate the early history of the Moon [1] leading to kilometer scale topographic variations on the lunar surface, with smaller crater [2], progressively introducing higher frequency topography. Crater wall slopes represent most of the overall topographic variation since many locations on the Moon are craters. While impact events lead to the formation of steep slopes [3], they are also primarily responsible for landform degradation [4]. During crater formation, target properties and processes controlling structural stability limit maximum slopes [4]. Younger craters have steeper slopes, but over time impact-induced degradation at multiple scales reduce slopes [4]. Decrease in crater wall slope with crater age has been discussed in past work, but mostly in the context of smaller (D<5 km) craters [5], younger simple craters [6], or implicit in the study of simple crater shape degradation [7]. Past work analyzing complex crater wall slopes is sparse, owing partly to the difficulty in characterizing crater wall slopes in the presence of terraces, slumps, large blocks etc. and also due to the lack of global topographic data before Lunar Reconnaissance Orbiter and Kaguya. In this work we characterize wall slope and local topographic heterogeneity for 44 complex craters (Copernican and Non-Copernican) to investigate the relation between slope and age.

**Methods:** A simple approach is adopted in this work to compare slopes of large complex craters with absolute model ages (AMAs). Since steeper slopes degrade faster than shallower slopes over time (due to existing slopes supporting fast downslope removal) [12], the $90^{th}$ percentile statistics, which represent steep or high slope values, were obtained for both wall slope and terrain ruggedness index (TRI, a measure for local topographic heterogeneity).

Topography was obtained from Lunar Reconnaissance Orbiter Camera (LROC) Wide Angle Camera (WAC) Global Mosaic Digital Terrain Model (DTM) sampled at 400 m/pixel [13]. Crater topography is characterized from a square area three times the crater's diameter, with the crater at the center. From these areas, each crater wall was manually digitized to obtain a mask to isolate and extract slope and TRI values, and obtain the 90th percentile statistics. Slope and TRI, the chosen topographic parameters, were computed from 3x3 pixel (1200 m by 1200 m) areas.

Table 1: List of complex craters. *Copernican craters

| Crater | D (km) | Model Age (Ga) | Lon | Lat |
|---|---|---|---|---|
| Moore F* | 24 | 0.041∓0.012 [8] | 37.30 | 185.0 |
| Wiener F* | 30 | 0.017∓0.002 | 149.97 | 40.90 |
| Klute W* | 31 | 0.090∓0.007 | 216.70 | 37.98 |
| Necho* | 37 | 0.080∓0.024 [8] | 123.3 | –5.3 |
| Aristarchus* | 40 | 0.175∓0.009[5] | 312.5 | 23.7 |
| Jackson* | 71 | 0.147∓0.038 [9] | 196.7 | 22.1 |
| McLaughlin | 75 | 3.7∓0.1 [10] | 267.17 | 47.01 |
| Pitiscus | 80 | 3.8∓0.1 [10] | 30.57 | -50.61 |
| Al-Biruni | 80 | 3.8∓0.1 [10] | 92.62 | 18.09 |
| La Pérouse | 80 | 3.6∓0.1 [10] | -10.66 | 76.18 |
| Birkeland | 82 | 3.8∓0.1 [10] | 174.01 | -30.17 |
| Bridgman | 82 | 3.9∓0.1 [10] | 136.98 | 43.39 |
| Geminus | 82 | 3.2∓0.4 [10] | 56.66 | 34.42 |
| Lyman | 83 | 3.5∓0.1 [10] | 162.47 | -64.96 |
| Ioffe | 84 | 3.6∓0.1 [10] | 230.85 | -14.38 |
| Tikhov | 84 | 3.8∓0.1 [10] | 172.29 | 61.66 |
| Neumayer | 84 | 4.0∓0.1 [10] | 70.92 | -71.16 |
| Hale | 84 | 3.3∓0.2 [10] | 91.71 | -74.13 |
| Freundlich | 85 | 4.0∓0.1 [10] | 170.89 | 25.07 |
| Paracelsus | 86 | 3.8∓0.1 [10] | 163.44 | -22.92 |
| Tycho* | 86 | 0.085∓0.018 [11] | 348.78 | -43.30 |
| Hayn | 86 | 1.8∓0.4 [10] | 83.87 | 64.56 |
| Lobachevskiy | 87 | 3.8∓0.1 [10] | 113.07 | 9.76 |
| Hahn | 88 | 3.8∓0.1 [10] | 73.55 | 31.22 |
| Aristoteles | 88 | 2.7∓0.8 [10] | 17.32 | 50.24 |
| Piccolomini | 89 | 3.9∓0.1 [10] | 32.2 | -29.7 |
| Laue | 89 | 3.9∓0.1 [10] | 262.95 | 28.29 |
| Vlacq | 89 | 3.9∓0.1 [10] | 38.69 | -53.39 |
| Roberts | 89 | 3.9∓0.1 [10] | 185.75 | 70.66 |
| Baillaud | 89 | 3.9∓0.1 [10] | 37.35 | 74.61 |
| Coulomb | 90 | 3.7∓0.1 [10] | 54.46 | 244.99 |
| Robertson | 90 | 3.7∓0.1 [10] | 254.64 | 21.84 |
| Ansgarius | 91 | 3.9∓0.1 [10] | 79.72 | -12.92 |
| Langmuir | 92 | 3.5∓0.1 [10] | 231.10 | -35.85 |
| Bose | 93 | 3.8∓0.1 [10] | 190.63 | -53.95 |
| Arnold | 93 | 3.8∓0.1 [10] | 35.83 | 66.98 |
| Icarus | 94 | 3.8∓0.1 [10] | 186.74 | -5.49 |
| Manzinus | 96 | 3.8∓0.1 [10] | 26.37 | -67.51 |
| Copernicus* | 97 | 0.797∓0.052 [11] | 339.92 | 9.62 |
| Joule | 98 | 4.0∓0.1 [10] | 215.87 | 27.15 |
| Vestine | 98 | 3.8∓0.1 [10] | 93.68 | 33.87 |
| Vavilov | 98 | 1.7∓0.1 [10] | 221.22 | -0.87 |
| Theophilus | 99 | 3.0∓0.6 [10] | 26.28 | -11.45 |
| Hausen | 163 | 3.5∓0.1 [10] | 271.51 | -65.11 |

**Results and discussions:** Slope distributions show that the dataset can be divided into 3 major populations, coinciding with geologic ages. Copernican craters have the higher slope values (Moore F, Wiener F, Klute W, and Necho have median slope values >30°(Figure

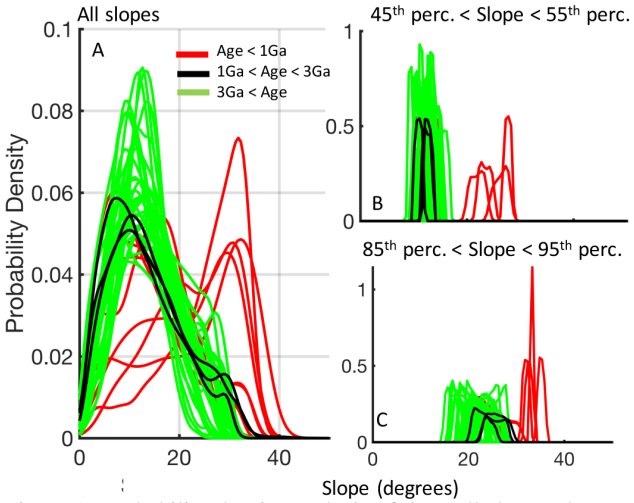


Figure 1: Probability density analysis of the wall slope value of each complex crater.

1a), followed by craters with ages between 1 Ga and 3 Ga and finally by craters with age > 3 Ga, although the slope distributions overlap. However, considering slopes around the median ($45^{th}$ to $55^{th}$ percentile; Figure 1B) improves the separation between Copernican and Non-Copernican craters. Further de-clustering of the age groups is achieved by considering slopes around the $90^{th}$ percentile ($85^{th}$ to $95^{th}$ percentile; Figure 1C). $90^{th}$ percentile slope values are used in this work, at even higher percentiles, the data density is much lesser. At the 90th slope percentile, the three different populations are grouped in their respective age sequence.

Our analysis shows that between 0 - 1 Ga (Figures 2a,b), slope approximates age. Copernican craters show a strong exponential decay with the power function of $f(x) = 62.3x^{-0.164}$ and an $R^2$ of 0.66 (Figure 2a inset). Beyond 1 Ga, there is a slope-age variant, but is it is not a clear line. There appears to be a disconnect in the slope-age plot outside of the Copernican range (Figures 2a,b). Non-Copernican craters flat-line around 3-1 Ga, before expressing an ambiguous trend through 4 Ga. With a baseline of 1.2 km in our set of complex craters, we find TRI and slope are strongly correlated ($R^2 = 0.99$) and are related linearly (Slope = 0.016TRI - 0.04), thus, no additional information is available from TRI.

**Conclusion:** We show that slope at $90^{th}$ percentile is an important measure of crater age, and correlates well for Copernican craters. Future work will be expanded with a detailed analysis and modeling of wall slope distributions from complex craters to estimate age.

**References:** [1] P. H. Schultz, et al. (1975) *Earth, Moon, and Planets* 12(2):159. [2] M. A. Kreslavsky, et al. (2013) *Icarus* 226(1):52. [3] D. E. Gault, et al. (1978) in *LPSC Proceedings* vol. 9 3843–3875. [4] J. W. Head (1975)

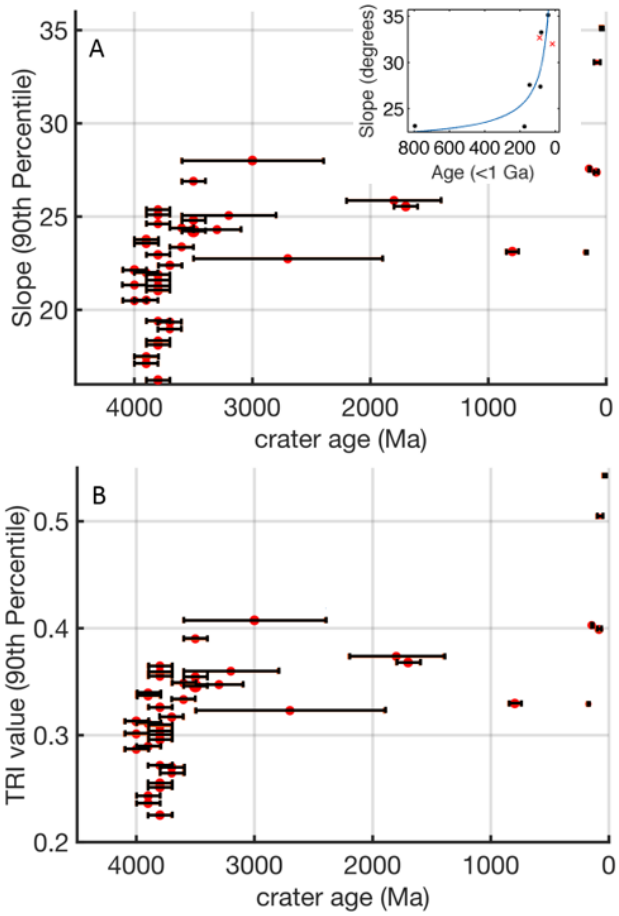


Figure 2: Slope (A) and TRI (B) values as a function of age. Inset 2A shows line of fit for craters <1000 Ma.

*Moon* 12:299. [5] R. Pike (1977) in *LPSC Proceedings* vol. 8 3427–3436. [6] L. A. Soderblom (1970) *J Geophys Res* 75(14). [7] L. A. Soderblom, et al. (1972) *J Geophys Res* 77(2). [8] T. Morota, et al. (2009) *Geophys Res Lett* 36(21). [9] C. Van derBogert, et al. (2010) in *LPSC* vol. 41 2165. [10] M. R. Kirchoff, et al. (2013) *Icarus* 225(1):325. [11] H. Hiesinger, et al. (2012) *J Geophys Res: Planets* 117(E12). [12] H. P. Ross (1968) *J Geophys Res* 73(4):1343. [13] F. Scholten, et al. (2012) *J Geophys Res: Planets* 117(E12).